

CONTROLLING THE DEVELOPMENT OF STATIONARY LONGITUDINAL STRUCTURES IN THE BOUNDARY LAYER ON A FLAT PLATE USING RIBLETS

D. S. Lokhov, A. V. Boiko, and D. S. Sboev

UDC 532.526

This paper reports results of experiments on controlling longitudinal structures in the boundary layer on a flat plate. The longitudinal structures were generated by a controlled vortical disturbance of the external flow by means of a distributed susceptibility mechanism. It is shown that riblets reduce the intensity of both stationary and traveling disturbances. The linear and weakly linear stages in the development of disturbances in the boundary layer are the most favorable for the use of riblets.

Key words: *boundary layer, distributed susceptibility, longitudinal structures, control, riblets.*

Introduction. It is known that in many cases, laminar–turbulent transitions are dominated by longitudinal structures. An example is a transition under conditions of elevated free-stream turbulence. Subsequently, the longitudinal structures that arise in this case undergo secondary instability, resulting in turbulent spots [1].

At present, the mechanisms of occurrence of longitudinal structures in boundary layers as primary instability under natural conditions have not been clarified. Model experiments have shown that generation of these disturbances by external turbulence can be implemented by means of both localized [2] and distributed [3, 4] susceptibilities.

There have been few experiments on controlling the development of longitudinal structures in boundary layers. Katasonov and Kozlov [5] employed a method of active control of longitudinal structures localized in space and time (so-called puffs) using localized injection–suction through a hole in the wall. In [6], the growth of these disturbances was suppressed by wall oscillations in the transverse direction, and in [7] by means of riblets. Studies have been performed of the effect of riblets on longitudinal vortices generated using roughness elements in the boundary layer on a flat plate [8] and on an oblique wing [9]. These studies were successful in the sense that a decrease in disturbance energy was achieved using control. It should be noted that all these experiments dealt with controlling disturbances generated by localized susceptibility mechanisms.

The distributed generation of a stationary longitudinal structure in a laminar boundary layer on a flat plate was studied in detail in [3, 4]. The data of these experiments are in good agreement with the results of theoretical papers [10–12]. In contrast to localized generation, distributed susceptibility ensures a continuous energy flow from external disturbances to disturbances inside the boundary layer [13], which can reduce the control effectiveness. Research on the control of the disturbances resulting from distributed susceptibility has not yet been performed and is therefore very important.

Riblets, as is known, are a longitudinal ribbing of a body surface and are an effective passive means for controlling the boundary layer in both turbulent flows [14] and in the early nonlinear stages of laminar–turbulent transitions [15]. Their advantages are ease in manufacturing and stability against external action. Laminar–turbulent transitions under high free-stream turbulence conditions are frequently encountered in problems of internal aerodynamics, for examples in designing gas-turbine blades. Various unfavorable factors (such as high temperatures

Institute of Theoretical and Applied Mechanics, Siberian Division, Russian Academy of Sciences, Novosibirsk 630090; denis.lokhov@gmail.com; sboev@itam.nsc.ru. Translated from *Prikladnaya Mekhanika i Tekhnicheskaya Fizika*, Vol. 46, No. 4, pp. 47–54, July–August, 2005. Original article submitted June 7, 2004.

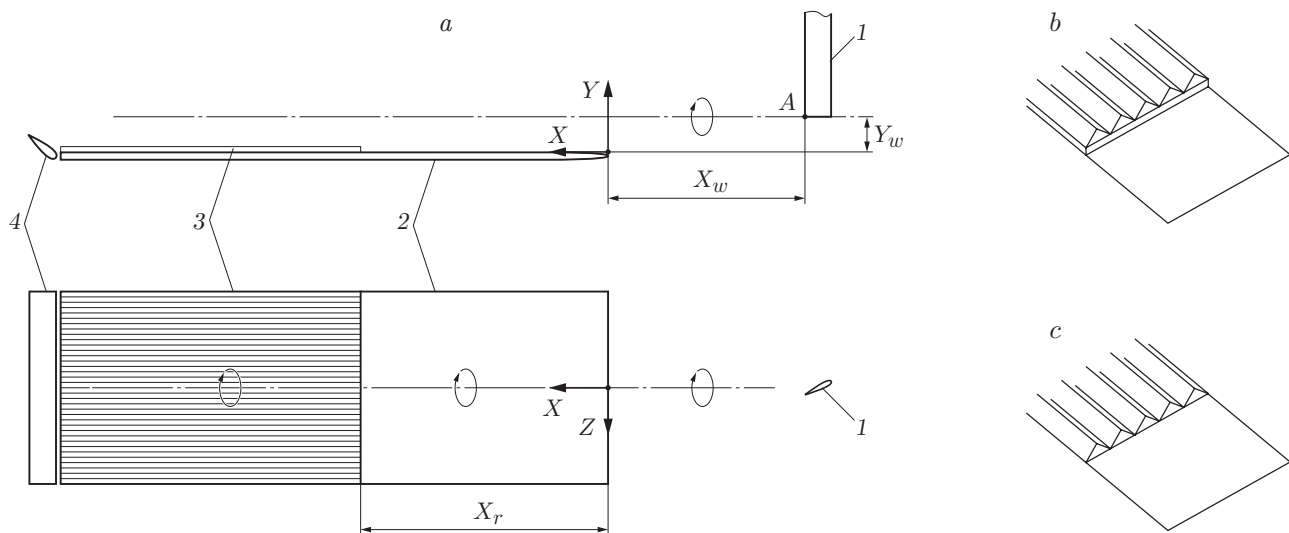


Fig. 1. Diagram of experiment (a) and mounting of riblets (b and c): 1) microwing; 2) flat plate; 3) riblets; 4) flap.

of the external flow and high heat fluxes to the wall) can hamper the use of active control methods. These circumstances motivated the choice of riblets as the main flow control method in the present study.

Experimental Technique. The experiments were performed in the MT-324 wind tunnel of the Institute of Theoretical and Applied Mechanics, Siberian Division of the Russian Academy of Sciences. The external-flow turbulence level did not exceed 0.1%. The model was a flat Plexiglas plate with dimensions of $700 \times 200 \times 10$ mm placed in the working section of the tube at zero angle of attack. The leading edge of the plate consisted of two semiellipses with an axis ratio of $132 : 8$ mm for the lower surface and $132 : 2$ mm for the upper edge. The pressure gradient above the surface of the model was controlled using the flap fixed at the trailing edge.

The experiments were performed under controlled conditions. The method for generating a stationary longitudinal structure in the boundary layer is similar to that first used in [3] and consists of the following. Ahead of the leading edge of the model and above its surface there is a microwing which is fixed upright at a certain angle of attack on the upper wall of the working section of the tunnel (Fig. 1). As is shown in [3], the interaction of the boundary layer with the vortex trailing from the free tip of the microwing and developing above the plate surface in the external flow leads to the occurrence of a stationary longitudinal structure inside the layer. Since the trailing vortex is stationary, it provides distributed generation of disturbances in the boundary layer, which is also confirmed by the data of [4]. The main mechanism of generation of the longitudinal structure is the so-called lift-up effect [1, 16]. The intensity of the trailing vortex and the longitudinal structure can be controlled by varying the angle of attack of the microwing and the flow velocity.

The following coordinate system is used: the X axis is directed downstream, the Y axis is perpendicular to the plate surface, and the Z axis is parallel to the leading edge of the plate. The origin is opposite to the vortex-forming tip of the microwing on the leading edge of the plate.

The present paper gives the results of two series of measurements, which differed in the type of microwing used, the method of mounting riblets, and the free-stream velocity. In the first series of experiments, we used a FXL V152 laminarized Wortmann airfoil microwing with a with a chord of 5 mm and 0.6 mm thick (Fig. 2). This microwing was also used in [4]. The free-stream velocity was $U_0 = 7.5$ m/sec. In the second series of experiments, we used a microwing designed by us, whose airfoil is shown in Fig. 2. The chord of this microwing was 6 mm, and the thickness was 0.7 mm. In this series of experiments, the free-stream velocity for two regimes was 4.2 and 6 m/sec. The distances from the vortex-forming wing (the coordinates of the point A in Fig. 1a) to the leading edge of the model are indicated in Table 1.

In these experiments, riblets designed by Grek et al. [15] were used. They had the shape of a thin coating with parallel grooves of triangular section (with apex angles of about 60°) on the surface. Riblets 1 mm high covered the plate over the entire width, and the grooves were directed streamwise. The two series of experiments differed in

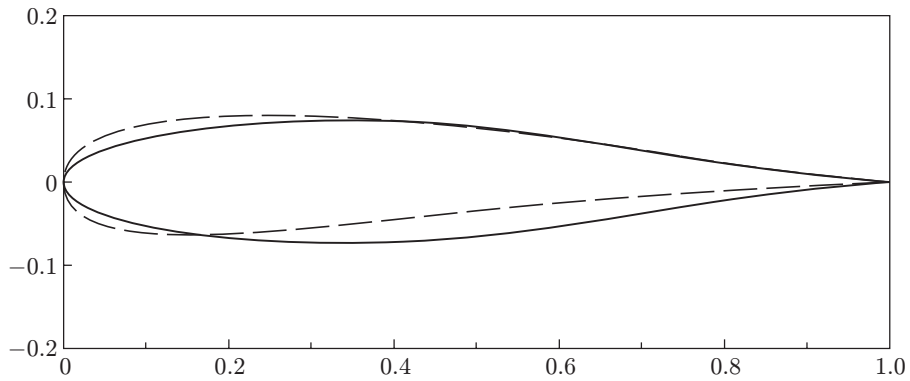


Fig. 2. FXL V152 airfoil (solid curve) and the microwing airfoil designed by the authors (dashed curve).

TABLE 1

| Series of experiments | X_w , mm | Y_w , mm | X_r , mm |
|-----------------------|---------------|---------------|---------------|
| First | 100 | 15 | 220 |
| Second | 112 | 12 | 150 |

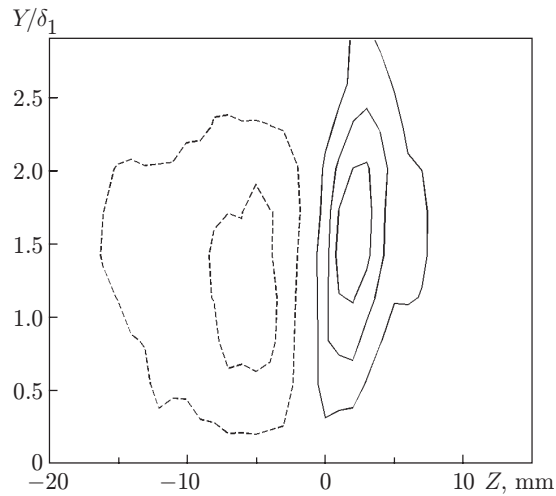


Fig. 3. Isolines of the mean velocity defect in the boundary layer for $X = 200$ mm: the solid curves are negative deviations and the dashed curves are positive deviations.

the way the riblets were mounted. In the first series, the riblets were mounted on the model in such a manner that a step formed between the riblet base and the surface of the smooth model (see Fig. 1b). In the second series, the base was flush-mounted in the model and only the ribs protruded above its surface (see Fig. 1c). The coordinates of the beginning of the ribbed surface for both series of measurements are also indicated in Table 1.

The longitudinal component of the flow velocity was measured by a single-wire hot-wire probe. The output data of the probe were digitized by a 12-digit analog-to-digital converter, linearized, and sent to a computer for further processing with a MatLab software package. The traverse gear used to move the sensor allowed three-dimensional measurements with an accuracy of 0.1 mm along the X and Z axes and 0.01 mm along the Y axis.

First Series of Experiments. Figure 3 shows isolines of the mean velocity defect in the disturbed boundary layer above the smooth model at $X = 200$ mm. These distributions are obtained by subtraction of the mean velocity

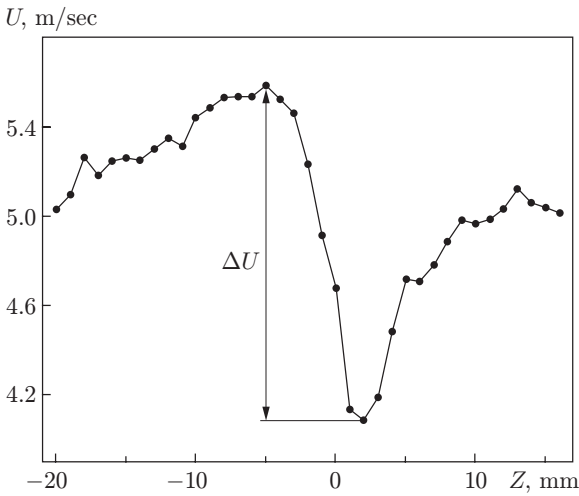


Fig. 4

Fig. 4. Mean velocity distribution for $X = 200$ mm and $Y/\delta_1 = 1.4$.

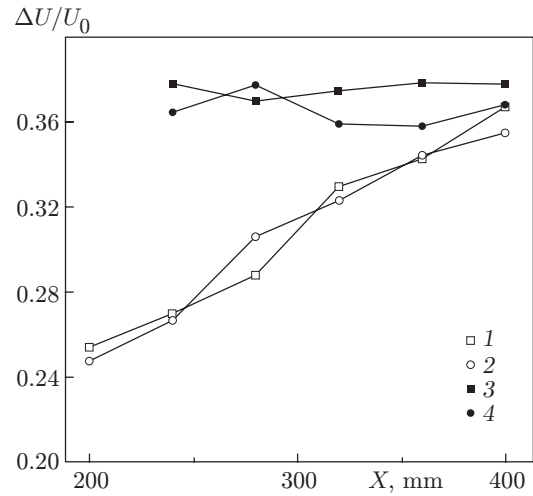


Fig. 5

Fig. 5. Stationary disturbance magnitude above the smooth surface (points 1 and 2) and above the ribbed surface (points 3 and 4) versus the longitudinal coordinate.

profiles in the undisturbed flow from the same profiles measured in the disturbed boundary layer. It is evident that in the plane (Y, Z) , the examined stationary disturbance consists of two closely spaced regions of positive and negative velocity defects localized on the transverse coordinate, and the disturbance maximum is at $Y/\delta_1 \approx 1.3-1.5$, where δ_1 is the displacement thickness of the undisturbed boundary layer. The results obtained for the smooth plate are in good agreement with the data of [4]. This indicates that a stationary longitudinal structure was generated in the boundary layer by means of a distributed susceptibility mechanism. In [4], data from measurements in the tip vortex of the same microwing for approximately the same angle of attack and free-stream velocity are given and it is shown that this vortex is laminar. In addition, measurements of velocity oscillation in the boundary layer have not revealed differences from the undisturbed flow.

The simplest method for estimating the disturbance growth is the use of the so-called magnitude $\Delta U = U_{\max} - U_{\min}$, i.e., the difference between the maximum and minimum values in the velocity distributions on the transverse coordinate measured for various values of X and $Y/\delta_1 = \text{const}$. An example of such a distribution is shown in Fig. 4. In this series of experiments, measurements were performed for $Y/\delta_1 = 1.4$.

The growth in the stationary disturbances on the smooth model is shown in Fig. 5 (points 1 and 2 correspond to the data obtained in two independent measurements). This allows the reproducibility of the results to be considered good. It is evident that the distortion of the disturbance increases linearly with increase in the longitudinal coordinate. In the measured range of X , the values of $\Delta U/U$ reach approximately 37%. The linear increase in the magnitude is in good agreement with the results of [3, 4, 10]. Figure 5 also gives curves of the magnitudes of the longitudinal structure above the ribbed surface versus the longitudinal coordinate obtained in two independent measurements (points 3 and 4). As follows from these curves, the riblets prevent the disturbances from increasing downstream, but in this series of experiments there was a considerable increase in the disturbance magnitude in the case of using riblets. It was assumed that this increase in the magnitude could be caused by the effect of the step that formed between the riblet base and the surface of the model. Such a situation is described, for example, in [15]. To verify this assumption, we performed a second series of experiments, in which as noted above, the base riblets was flush-mounted in the model.

Second Series of Experiments. In addition to the difference in the method of mounting riblets, in this series of experiments, we used a microwing of different design and different airfoil, in which the cross section of the maximum relative thickness of this airfoil is shifted to the tip compared to the Wortmann laminarized airfoil (see Fig. 2). As is known [17], large lift coefficients (and, consequently, trailing vortices of sufficient intensity) for such airfoils are observed in regimes where flow with a separation bubble and subsequent attachment of the

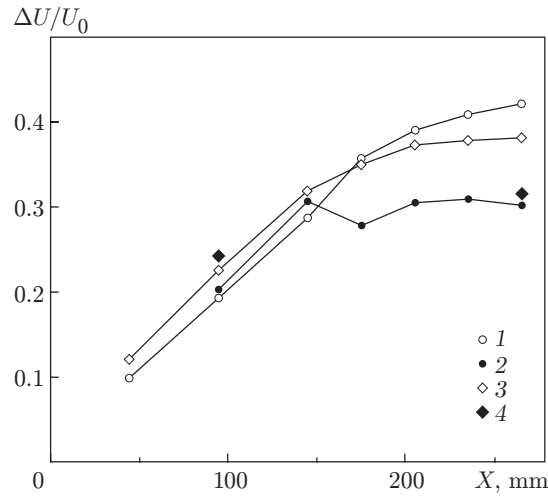


Fig. 6. Stationary disturbance magnitude above the smooth surface (points 1 and 3) and above the ribbed surface (points 2 and 4) versus longitudinal coordinate for $U_0 = 4.2$ (1 and 2), and 6 m/sec (3 and 4).

turbulent boundary layer occurs on the upper face of the airfoil. For this reason, the trailing vortex in this series of experiments was turbulent. The oscillation intensity of the longitudinal velocity components above the outer edge of the boundary layer under the vortex core (at $Z = 4$ mm) was 1.6% at $X = 45$ mm and 1.3% at $X = 265$ mm.

In this case, as in the first series of experiments, the stationary disturbance consisted of two and closely spaced regions of positive and negative velocity defects on the transverse coordinate. Both the distributed generation of stationary longitudinal structures and the continuous exposure of the boundary layer to nonstationary gave rise led to some differences in the development of disturbances inside the layer. In particular, in this case, the nonstationary disturbances inside the boundary layer also increased downstream. The interaction of the stationary longitudinal structure and traveling disturbances in the boundary layer led to nonlinear development of the longitudinal structure and the occurrence of secondary instability. A detailed description of these processes is beyond the scope of this paper. We note, however, that secondary instability in this case was manifested in disturbance of the linear increase in the magnitude of the longitudinal structure due to the attainment of saturation of the longitudinal coordinate (points 1 and 3 in Fig. 6), a rapid increase in high-frequency disturbances downstream, and the subsequent occurrence of a turbulent wedge. As the local Reynolds number increased with increase in the free-stream velocity, the beginning of these processes shifted upstream and secondary instability occurred at a smaller magnitude of the longitudinal structure.

Curves of the stationary disturbance magnitude versus the longitudinal coordinate for the smooth and ribbed models are given in Fig. 6. The measurements were performed for $Y/\delta_1 = 1$. We recall that in this case the leading edge of the riblets is at a distance $X = 150$ mm. The results obtained at $X = 95$ mm, i.e., above the smooth surface show good reproducibility of the measurements. In Fig. 6 it is evident that in this case, as in the previous case, the use of riblets stops the downstream growth of the magnitude (point 2). However, the effect of the base is not observed and the magnitude of the longitudinal structure is always smaller on the ribbed surface than on the smooth surface.

It is interesting that an increase in U_0 reduces the effectiveness of suppressing the longitudinal structure by the riblets. This follows from the data obtained at $X = 265$ mm (Fig. 6): for $U_0 = 4.2$ m/sec, the magnitude on the ribbed surface decreased by 29%, and for $U_0 = 6$ m/sec, it decreased by 15%. The main difference between these regimes is that the nonlinear development of the longitudinal structure begins earlier as free-stream velocity increases. In Fig. 5 it is evident that for $U_0 = 4.2$ m/sec on the smooth model, the nonlinear saturation stage begins at $X > 175$ mm, i.e., in this case, the riblets initially affect the structure which is at a linear stage of development. An increase in U_0 , as was noted above, leads to an upstream shift of the location of the beginning of the nonlinear stage ($X > 145$ mm for $U_0 = 6$ m/sec), and in this case, the riblets affect the disturbance which is already developing nonlinearly.

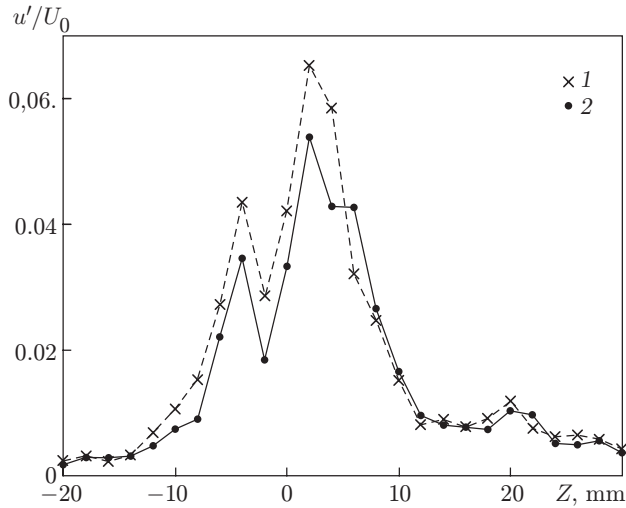


Fig. 7

Fig. 7. Distributions of the mean square amplitude of boundary-layer oscillations above the smooth surface (points 1) and above the ribbed surface (points 2) at $X = 265$ mm and $U_0 = 4.2$ m/sec.

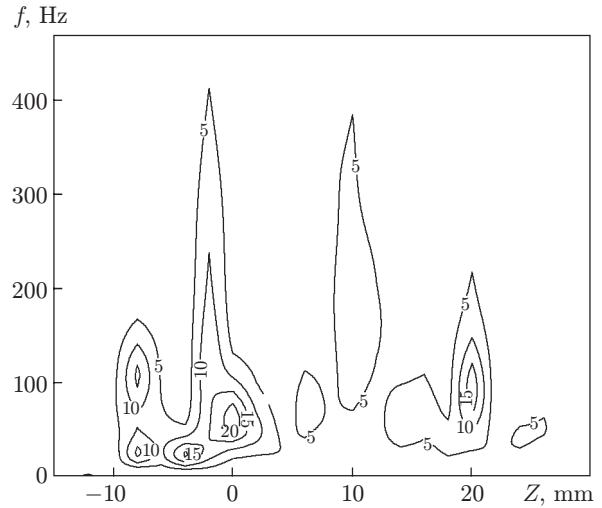


Fig. 8

Fig. 8. Isolines of the damping coefficient of traveling disturbances above the ribbed surface at $X = 265$ mm and $U_0 = 4.2$ m/sec.

Figure 7 gives distributions of the integral (over the spectrum) mean square amplitude of boundary-layer oscillations above the smooth and ribbed surface at $U_0 = 4.2$ m/sec and $X = 265$ mm. For the smooth surface, these data were obtained in the regime of intensely developing secondary instability. The peaks in the oscillation distributions correspond to the locations of the greatest gradients of the mean velocity on the transverse coordinate, which is in good agreement with the well-known results on secondary instability of longitudinal structures [1, 9]. It is evident that above the ribbed surface, the integral (over the spectrum) oscillation amplitude decreases. Figure 8 gives curves of the damping coefficient versus the transverse coordinate in the form of isolines for various frequencies. The greatest damping (by a factor of 10–20) is observed of disturbances with a frequency of 20 to 250 Hz localized inside the stationary longitudinal structure (-10 mm $< Z < 5$ mm), i.e., those that develop because of its secondary instability. This result is similar to that obtained in [9] for a packet of instability waves that develops in a stationary longitudinal vortex above a ribbed oblique wing. The damping of high-frequency oscillations is due to a decrease in the mean velocity gradient on the transverse coordinate in the stationary longitudinal structure above the ribbed surface compared to the smooth surface. The relatively small decrease in the oscillation amplitude which is integral over the spectrum (see Fig. 7) is due to the fact that the disturbances with a frequency of up to 10 Hz, which dominate in the spectra, damp very weakly above the ribbed surface.

Conclusions. It was shown that riblets can be successfully used to control longitudinal structures generated in a boundary layer by means of a distributed susceptibility mechanism. Such control can be applied to both laminar longitudinal structures and to disturbances of the indicated type at a nonlinear stage of development. In the latter case, the control is less effective. If riblets are used at the stage of secondary instability, they can have a favorable effect by suppressing high-frequency oscillations that develop inside longitudinal structures.

We thank V. V. Kozlov for useful discussions of the results and course of the experiments.

This work was supported by the Russian Foundation for Basic Research (Grant No. 02-01-00006), the Foundation “Leading Scientific Schools of Russia” (Grant No. NSh-964.2003.1) and the INTAS International Foundation (Grant No. 00-00323).

REFERENCES

1. A. V. Boiko, G. R. Grek, A. V. Dovgal', and V. V. Kozlov, *Occurrence of Turbulence in Wall Flows* [in Russian], Nauka, Novosibirsk (1999).
2. A. V. Boiko, G. R. Grek, and D. S. Sboev, "Spectral analysis of localized disturbances in boundary layer at subcritical Reynolds numbers," *Phys. Fluids*, **15**, No. 12, 3613–3624 (2003).
3. F. P. Bertolotti and J. M. Kendall, "Response of the Blasius boundary layer to controlled free-stream vortices of axial form," AIAA Paper No. 97-2018, New York (1997),
4. A. V. Boiko, "Susceptibility of the boundary layer of a flat plate to a stationary vortical disturbance of the external flow," *Izv. Ross. Akad. Nauk, Mekh. Zhidk. Gaza*, No. 6, 71–82 (2001).
5. M. M. Katasonov and V. V. Kozlov, "Active control of longitudinal structures in boundary layers," in: *Abstracts of the 3rd Int. Workshop on Stability of Homogeneous and Heterogeneous Liquids* (Novosibirsk, April 24–26, 1996), Inst. of Theor. and Appl. Mech., Sib. Div., Russian Acad. of Sci., Novosibirsk (1996), pp. 44–46.
6. M. M. Katasonov and V. V. Kozlov, "Effect of transverse vibrations of a surface on the development of longitudinal laminated structures and incipient turbulent spots," Preprint No. 5-97, Inst. of Theor. and Appl. Mech., Sib. Div., Russian Acad. of Sci., Novosibirsk (1997).
7. P. H. Alfredsson, A. A. Bakchinov, M. M. Katasonov, and V. V. Kozlov, "Control of laminar–turbulent transition with high free-stream turbulence by means of localized suction," Preprint No. 4-98, Ins. of Theor. and Appl. Mech., Sib. Div., Russian Acad. of Sci., Novosibirsk (1998).
8. G. R. Grek, V. V. Kozlov, S. V. Titarenko, and B. G. B. Klingmann, "The influence of riblets on a boundary layer with embedded streamwise vortices," *Phys. Fluids A.*, **7**, No. 10, 2504–2506 (1995).
9. A. V. Boiko, V. V. Kozlov, V. V. Syzrantsev, and V. A. Shcherbakov, "Control of laminar–turbulent transition in a stationary oblique-wing vortex using riblets," *Teplofiz. Aéromekh.*, **3**, No. 1, 82–94 (1996).
10. F. P. Bertolotti, "Response of the Blasius boundary layer to freestream vorticity," *Phys. Fluids*, **9**, No. 8, 2286–2299 (1999).
11. P. Luchini, "Reynolds-number-independent instability of the boundary layer over a flat surface: Optimal perturbations," *J. Fluid Mech.*, **404**, 289–309 (2000).
12. P. Andersson, M. Berggren, and D. S. Henningson, "Optimal disturbances and bypass transition in boundary layers," *Phys. Fluids*, **11**, No. 1, 134–150 (1999).
13. Yu. S. Kachanov, V. V. Kozlov, and V. Ya. Levchenko, *Occurrence of Turbulence in a Boundary Layer* [in Russian], Nauka, Novosibirsk (1982).
14. M. J. Walsh, "Riblets as a viscous drag reduction technique," *AIAA J.*, **21**, No. 4, 485–486 (1983).
15. G. R. Grek, V. V. Kozlov, and S. V. Titarenko, "An experimental study on the influence of riblets on transition," *J. Fluid Mech.*, **315**, 31–49 (1996).
16. M. T. Landahl, "Note on an algebraic instability of inviscid parallel shear flows," *J. Fluid Mech.*, **98**, 243–251 (1980).
17. D. Kuchemann, *Aerodynamic Design of Aircraft*, Pergamon Press, Oxford (1978).